European Journal of Medical Genetics 65 (2022) 104626

Contents lists available at ScienceDirect

European Journal of Medical Genetics

journal homepage: www.elsevier.com/locate/ejmg

Detailed prenatal and postnatal MRI findings and clinical analysis of RAF1 in Noonan syndrome

Kjell Helenius [a,d,*], Riitta Parkkola [b], Anita Arola [a], Ville Peltola [a,d], Maria K. Haanpää [c,d]

[a] Department of Paediatrics and Adolescent Medicine, Finland
[b] Department of Radiology, Finland
[c] Department of Genomics and Medical Genetics, Turku University Hospital, Finland
[d] University of Turku, Turku, Finland

ARTICLE INFO

Keywords:
Noonan syndrome
Fetal imaging
Brain MRI
Very preterm infant

ABSTRACT

Noonan syndrome is a genetically heterogeneous developmental disorder, which usually includes findings such as short stature, facial dysmorphia, cardiac abnormalities and a varying degree of intellectual disability. We present a unique case of a rare variant of Noonan syndrome in a very preterm female infant born at 28 + 4 gestational weeks, with abnormal radiological findings visible at fetal magnetic resonance imaging (MRI) and evolution of the brain lesions during infancy.

1. Introduction

Noonan syndrome is caused by genetic variants affecting the RAS-MAPK pathway(Gelb and Tartaglia, 2006). The estimated incidence is 1/1000 to 1/2500 live born infants(Roberts et al., 2013). Clinical manifestations are highly variable, and several genotype-phenotype associations have been reported. Over 60% of patients diagnosed with Noonan syndrome show variants in the *PTPN11* or *SOS1* genes, while variants in the RAF1 gene account for around 10%(Razzaque et al., 2007; Roberts et al., 2013). Variants in the RAF1 gene located in chromosome 3p25 cause RAF1-associated Noonan syndrome (OMIM #611553).

The prenatal phenotype of Noonan syndrome usually includes unspecific ultrasound findings such as polyhydramnios and increased nuchal translucency or other signs of lymphatic dysplasia(Gaudineau et al., 2013; Scott et al., 2021). Reported prenatal central nervous system findings include abnormalities of the posterior fossa and cerebral ventricles(Gaudineau et al., 2013; Lamouroux et al., 2022; Scott et al., 2021). Reports on postnatal central nervous system MRI findings in Noonan syndrome are scarce, but reported findings on brain MRI in RASopathies include cerebellar anomalies, delayed cortical gyration, white matter injuries and abnormalities of the corpus callosum(Cizmeci et al., 2018). To date, only few fetal MRI findings have been reported in postmortem case series(Lamouroux et al., 2022; Mastromoro et al., 2021).

This clinical report describes an interesting series of abnormal fetal and postnatal brain MRI findings in a live born patient diagnosed with RAF1-associated Noonan syndrome and associated severe cardiomyopathy.

2. Clinical report

Our patient is a female infant born to non-consanguineous parents of African and Caucasian descent. She was born vaginally at 28 + 4 gestational weeks due to spontaneous onset of preterm labor complicated by rapidly progressing polyhydramnios. Prenatal ultrasound examination showed nuchal hygroma (7–10 mm) at an estimated GA of 16 weeks and suspicion of hypoplastic vermis. Chromosomal microarray and trisomy-PCR testing were negative. Fetal MRI was performed at 22 + 0 gestational weeks using Siemens Avanto fit 1.5-T (T) MR scanner (Siemens Medical Imaging, Siemens Healthineers, Erlangen, Germany). The fetal MRI showed abnormalities in the central nervous system: delayed Sylvian fissure operculization and bilateral subdural effusion. In the posterior fossa, the vermis (height 8,9 mm, <10th percentile; width 5,2 mm, <3rd percentile) was hypoplastic (Fig. 1a–c.).(Kyriakopoulou et al., 2017)

At birth, the infant was hydropic (birth weight 1644 g, +3.5 SD) and needed immediate intubation and subsequently high frequency ventilation due to severe respiratory acidosis. Cranial ultrasound imaging on the day of birth showed sparse gyration, wide extracortical space and

* Corresponding author. Department of Paediatrics and Adolescent Medicine, Turku University Hospital, Savitehtaankatu 5, 20520, Turku, Finland.
E-mail address: kkhele@utu.fi (K. Helenius).

https://doi.org/10.1016/j.ejmg.2022.104626
Received 22 March 2022; Received in revised form 26 July 2022; Accepted 19 September 2022
Available online 22 September 2022

bilateral periventricular echolucency. Serial cranial ultrasound examination performed at 3 days of age confirmed these findings and showed a right-sided grade 1 germinal matrix hemorrhage. Echocardiogram on the second day of life showed echolucency in the atrioventricular valves but was otherwise normal. Serial echocardiograms were obtained due to the high probability of developing cardiac abnormalities and showed rapidly worsening findings of hypertrophic cardiomyopathy after the first week of life. Propranolol was initiated due to the associated risk of cardiac arrhythmias.

At 11 days of age the infant underwent brain MRI (Siemens Avanto fit 1.5-T (T) MR scanner), which demonstrated pathologic sulcal development. The sulci were smooth, and the operculum was open. All ventricles were wide and the cavum septum pellucidum was prominent. Hemosiderosis was seen bilaterally in the germinal matrix area. The ventricular ependyma showed marked signal loss representing hemoglobin break-down products. This phenomenon was also seen in the posterior fossa on the cerebellar surface. The tegmento-vermian angle was large (28°) and the vermis was hypoplastic (height 15 mm, width 9,4 mm, both <1st percentile)(Kyriakopoulou et al., 2017). Spectroscopy showed low NAA (N-Acetyl-Aspartate) at the level of thalamus on the right side (Fig. 2a–d).

Cranial ultrasound performed at 6 weeks of life showed persistently abnormal sulcal development and mildly enlarged lateral ventricles, but no other abnormalities.

At the age of 16 days the patient was referred to a medical geneticist. She was noted to have dysmorphic features: prominent, narrow forehead, short nose with anteverted nares and depressed nasal root, ocular hypertelorism, downslanting palpebral fissures, short neck (Fig. 3a); thick ear lobes, low-set and posteriorly rotated ears (Fig. 3b). Other abnormal findings included abnormally deep creases on the palms and soles (Fig. 3c and d). Clinical suspicion of RASopathy arose. An NGS-based analysis was performed with Sophia Genetics custom clinical exome solution including 4430 disease related genes and Illumina sequencing. Over 98% of target regions were covered with 50x. Variant annotation and filtering were performed with Sophia DDM and visualized with IGV (Broad Institute) The analysis revealed a known heterozygous pathogenic missense variant in the RAF1 gene, NM_002880.3 (RAF1):c.770C > T, p.(Ser257Leu), pathogenic (ACMG 5)(Kobayashi et al., 2010). The variant localizes in the important and conserved CR2 domain of the protein. Both parents were tested negative for this genetic variant, indicating a *de novo* mutational event.

The initial neonatal intensive care entailed early-onset *Escherichia coli* sepsis and meningitis, marked cardiac hypertrophy and the development of bronchopulmonary dysplasia. At the age of 8 weeks the infant was discharged to her local hospital for step-down care. She subsequently returned to our hospital due to two separate late onset episodes of *E. coli* meningitis, the latter of which included acute cardiac decompensation and evolution of obstructive hydrocephalus necessitating operative insertion of a ventriculo-peritoneal shunt. Postoperative brain MRI showed markedly restricted brain growth, periventricular leukomalacia, postoperative subdural effusions and satisfactory resolution of the ventricular enlargement (Fig. 4). Due to multiple episodes of gram-negative meningitis, whole-spine MRI was performed with normal findings. An immunologic evaluation revealed normal levels of neutrophils, lymphocyte subpopulations and immunoglobulins, but showed total deficiency of the complement lectin pathway and a partial

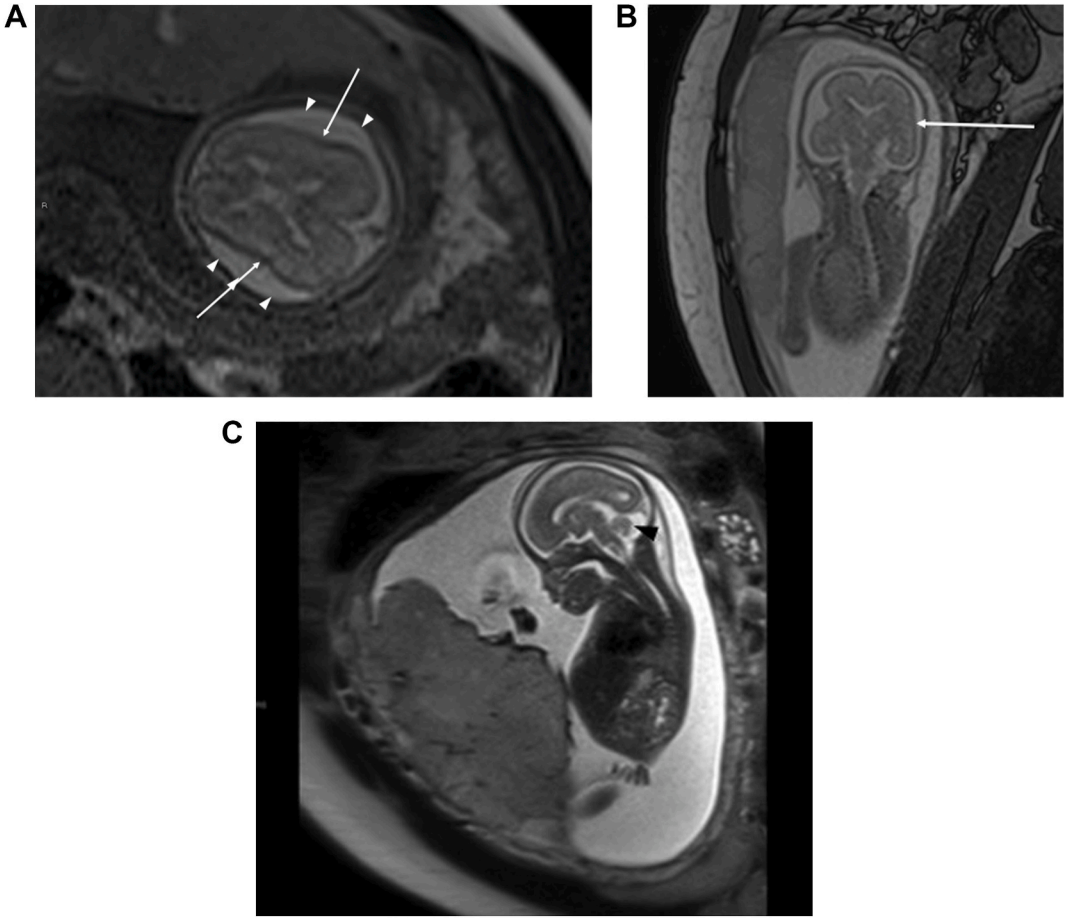

Fig. 1. Fetal MRI at 22 weeks of gestation showing abnormal brain findings in a very preterm infant diagnosed with Noonan syndrome. a) Axial T2 Haste. Bilaterally delayed Sylvian fissure operculization (long arrows) and bilateral subdural effusions (arrowheads)
b) Coronal T2 Trufi. Delayed Sylvian fissure operculization (long arrow) c) Sagittal T2 Haste. Hypoplastic cerebellar vermis (black arrowhead).

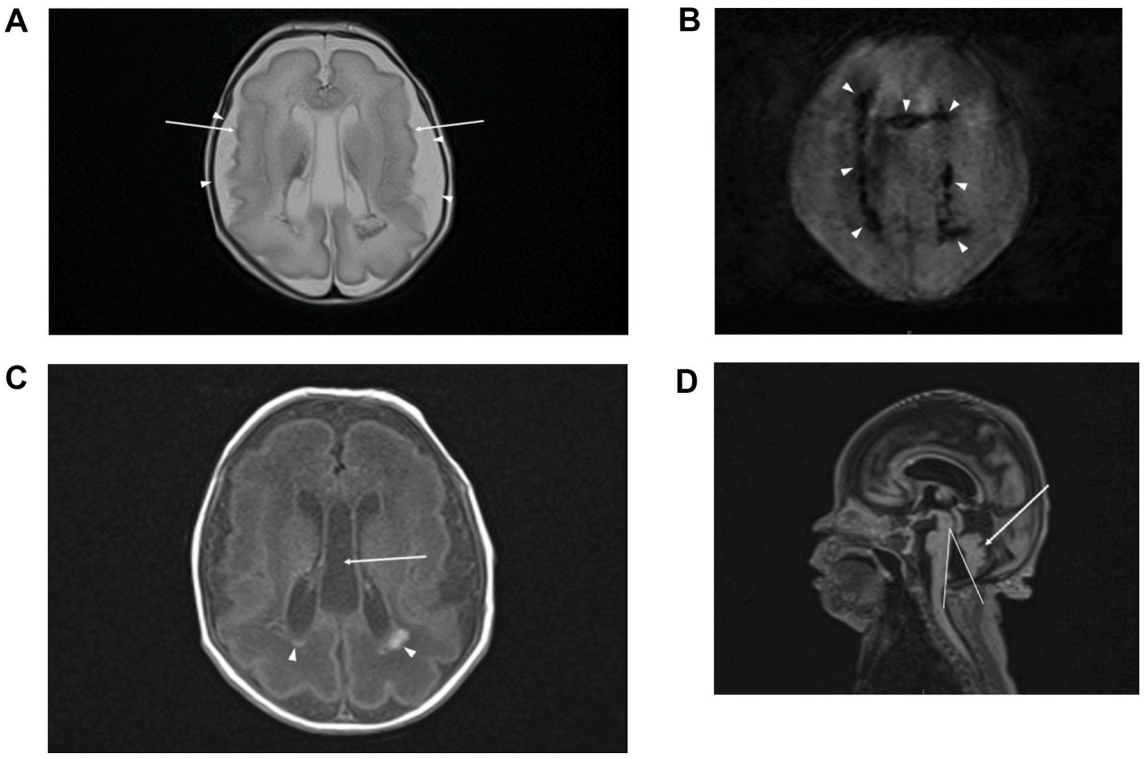

Fig. 2. Postnatal brain MRI at 11 days of age in a very preterm infant diagnosed with Noonan syndrome. a) Axial T2 Blade. Smooth cortical sulci and pathological Sylvian operculization (long arrows). Wide cortical subarachnoid spaces and prominent subdural spaces (arrowheads)
b) Axial SWI. Abundant hemoglobin break-down products on ependyma of lateral ventricles and on corpus callosum (arrowheads) c) Axial T1 SE. Wide cavum septum pellucidi cum cavum vergae (long arrow). Intracerebral hemorrhage occipitally under ependyma of the lateral ventricles (arrowheads) d) Sagittal 3D FLAIR. Hypoplastic vermis (long arrow) and large tegmento-vermian angle (angle).

deficiency of the alternate pathway. The level of properdin was about half of normal and the level of mannose binding lectin was low, caused by combined heterozygosity in the MBL2 gene (c.161G > A, p.(Gly54Asp) and c.170G > A, p.(Gly57Glu). She has subsequently received meningococcal quadrivalent conjugate vaccine and serogroup B vaccine, in addition to age-appropriate immunizations according to the national schedule.

At the age of 2 years, the motor development shows some delay, but good progress with regular physical therapy (self-ambulatory in lower positions, stable in upright position but not walking without support). Her feeding skills are close to age appropriate, and the feeding tube was removed at 7 months of age. Her growth chart shows normal weight (10,95 kg, −0,6SD) and head circumference (46,5 cm, −1,6SD), but stunted length (75,4 cm, −3,6SD). She has been diagnosed with bilateral moderate mixed type hearing deficit and uses hearing aids; verbal communication skills are delayed. Non-verbal communication skills are age appropriate. She required continuous home oxygen therapy due to prematurity-related severe bronchopulmonary dysplasia until approximately 12 months of age. Her cardiac function has remained stable during propranolol treatment, showing hypertrophic cardiomyopathy with moderate left outflow tract obstruction and normal cardiac function. No ocular or genitourinary abnormalities have been detected during follow-up.

3. Discussion

To our knowledge, this is the first report of the evolution of abnormal brain MRI findings in Noonan syndrome from fetal imaging to infancy. Our patient also developed hypertrophic cardiomyopathy, which is typical in RAF1-associated Noonan syndrome.

Prenatal suspicion of Noonan syndrome usually arises from a combination of unspecific signs such as polyhydramnios, lymphatic dysplasia and cardiac abnormalities on ultrasound imaging, but also brain findings such as hydrocephalus might be present(Gaudineau et al., 2013; Scott et al., 2021). It has been proposed that certain genotypes, such as RAF1 variants, might display more severe prenatal findings compared e.g. to the more common PTPN11 variants(Scott et al., 2021). The study by Scott et al. also showed that even if RAF1 variants are commonly associated with hypertrophic cardiomyopathy, this feature is rarely present prenatally, which also was the case with our patient.

Two recent postmortem (following termination of pregnancy) case reports describe fetal MRI imaging findings in Noonan syndrome (Lamouroux et al., 2022; Mastromoro et al., 2021). The main brain abnormalities described in these two cases are cerebellar abnormalities and external hydrocephalus, both of which were seen pre- and postnatally also in our patient. In contrast to these two previous reports, our patient also demonstrated delayed operculization of the Sylvian fissures, which has been found in patients with Noonan syndrome in postnatal MRI imaging.(Cizmeci et al., 2018). Interestingly, Cizmeci and colleagues also reported that intraventricular hemorrhage and white matter lesions are frequent in patients with Noonan syndrome. These abnormalities were found postnatally also in our patient, but we cannot necessarily attribute these to Noonan syndrome because of the effect of prematurity, sepsis and respiratory instability during postnatal stabilization, which are associated with intraventricular hemorrhage and periventricular leukomalacia(Volpe, 2009).

In addition to the fetal MRI findings, our patient had severe cardiac hypertrophy. The incidence of hypertrophic cardiomyopathy in Noonan syndrome varies depending on the genotype. The overall incidence of HCM in Noonan syndrome is approximately 20%, but in patients with RAF1 variants it is as high as 85%(Gelb et al., 2015). The overall 3-year survival prognosis of patients with HCM and Noonan syndrome is reported to be 74% but is markedly poorer if congestive heart failure develops(Wilkinson et al., 2012). Treatment of HCM is usually supportive,

Fig. 3. Photographs of dysmorphic features at 16 days of age in a very preterm infant diagnosed with Noonan syndrome (published with parental consent) a) Prominent, narrow forehead; short nose with anteverted nares and depressed nasal root; ocular hypertelorism; downslanting palpebral fissures b) Low-set, posteriorly rotated ears; thick earlobes c) Abnormally deep creases in the palms and soles.

with propranolol being the most commonly used medication. Our patient has remained under close cardiac follow-up, and her cardiac status is stable at 2 years of age. Lectin deficiency, which was diagnosed in our patient, is relatively prevalent in both Caucasian and sub-Saharan populations (5 and 10%, respectively) and is probably not related to Noonan syndrome(Degn et al., 2011).

Our case includes intriguing radiological abnormalities spanning from fetal imaging to infancy. This variant of Noonan syndrome is frequently complicated by hypertrophic cardiomyopathy, as in our patient. Immunological deficiencies are usually not associated with this syndrome. Our case reveals radiological findings evolving throughout the fetal and neonatal period and adds to the existing literature on central nervous system pre-and postnatal findings in patients with Noonan syndrome. The prognostic value of abnormal prenatal central nervous system findings and the potential genotype-phenotype correlation of such findings remains to be studied in larger patient series.

Funding sources

None received.

CRediT authorship contribution statement

Kjell Helenius: Corresponding author, Conceptualization, of the clinical report, Investigation, of the clinical data, Methodology, Writing – original draft, Writing – review & editing. **Riitta Parkkola:** Conceptualization, of the clinical report, Investigation, of the clinical data, Methodology, Writing – review & editing. **Anita Arola:** Conceptualization, of the clinical report, Investigation, of the clinical data, Methodology, Writing – review & editing. **Ville Peltola:** Conceptualization, of the clinical report, Investigation, of the clinical data, Methodology, Writing – review & editing. **Maria K. Haanpää:** Conceptualization, of the clinical report, Investigation, of the clinical data, Methodology,

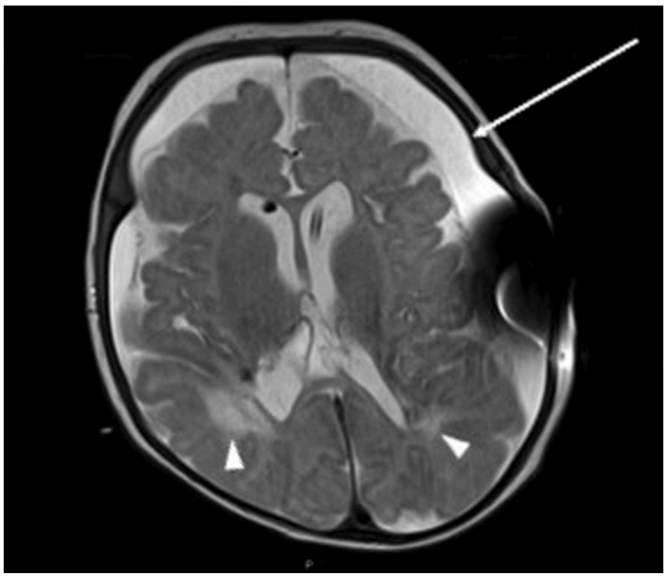

Fig. 4. Brain MRI at the age of 4 months in a very preterm infant diagnosed with Noonan syndrome. Axial T2 TSE. Restricted brain growth. Wide subdural spaces (long arrow). Periventricular leukomalacia (arrowheads).

Supervision, Writing – review & editing.

Declaration of competing interest

The authors report no conflicts of interest relevant to this report.

Data availability

The authors do not have permission to share data.

Acknowledgments

The authors wish to thank the patient's family for their collaboration with the publication of this clinical report.

References

Cizmeci, M.N., Lequin, M., Lichtenbelt, K.D., Chitayat, D., Kannu, P., James, A.G., Groenendaal, F., Chakkarapani, E., Blaser, S., de Vries, L.S., 2018. Characteristic MR imaging findings of the neonatal brain in RASopathies. Am. J. Neuroradiol. 39, 1146–1152. https://doi.org/10.3174/ajnr.A5611.

Degn, S.E., Jensenius, J.C., Thiel, S., 2011. Disease-causing mutations in genes of the complement system. Am. J. Hum. Genet. 88, 689. https://doi.org/10.1016/J.AJHG.2011.05.011.

Gaudineau, A., Doray, B., Schaefer, E., Sananès, N., Fritz, G., Kohler, M., Alembik, Y., Viville, B., Favre, R., Langer, B., 2013. Postnatal phenotype according to prenatal ultrasound features of Noonan syndrome: a retrospective study of 28 cases. Prenat. Diagn. 33, 238–241. https://doi.org/10.1002/PD.4051.

Gelb, B.D., Roberts, A.E., Tartaglia, M., 2015. Cardiomyopathies in Noonan syndrome and the other RASopathies. Prog. Pediatr. Cardiol. 39, 13. https://doi.org/10.1016/J.PPEDCARD.2015.01.002.

Gelb, B.D., Tartaglia, M., 2006. Noonan syndrome and related disorders: dysregulated RAS-mitogen activated protein kinase signal transduction. Hum. Mol. Genet. 15, R220. https://doi.org/10.1093/HMG/DDL197. –R226.

Kobayashi, T., Aoki, Y., Niihori, T., Cavé, H., Verloes, A., Okamoto, N., Kawame, H., Fujiwara, I., Takada, F., Ohata, T., Sakazume, S., Ando, T., Nakagawa, N., Lapunzina, P., Meneses, A.G., Gillessen-Kaesbach, G., Wieczorek, D., Kurosawa, K., Mizuno, S., Ohashi, H., David, A., Philip, N., Guliyeva, A., Narumi, Y., Kure, S., Tsuchiya, S., Matsubara, Y., 2010. Molecular and clinical analysis of *RAF1* in Noonan syndrome and related disorders: dephosphorylation of serine 259 as the essential mechanism for mutant activation. Hum. Mutat. 31, 284–294. https://doi.org/10.1002/humu.21187.

Kyriakopoulou, V., Vatansever, D., Davidson, A., Patkee, P., Elkommos, S., Chew, A., Martinez-Biarge, M., Hagberg, B., Damodaram, M., Allsop, J., Fox, M., Hajnal, J.v., Rutherford, M.A., 2017. Normative biometry of the fetal brain using magnetic resonance imaging. Brain Struct. Funct. 222, 2295. https://doi.org/10.1007/S00429-016-1342-6.

Lamouroux, A., Dauge, C., Wells, C., Mousty, E., Pinson, L., Cavé, H., Capri, Y., Faure, J. M., Grosjean, F., Sauvestre, F., Attié-Bitach, T., Pelluard, F., Geneviève, D., 2022. Extending the prenatal Noonan's phenotype by review of ultrasound and autopsy data. Prenat. Diagn. 42, 574–582. https://doi.org/10.1002/PD.6133.

Mastromoro, G., de Luca, A., Marchionni, E., Spagnuolo, A., Ventriglia, F., Manganaro, L., Pizzuti, A., 2021. External hydrocephalus as a prenatal feature of noonan syndrome. Ann. Hum. Genet. 85, 249–252. https://doi.org/10.1111/AHG.12436.

Razzaque, M.A., Nishizawa, T., Komoike, Y., Yagi, H., Furutani, M., Amo, R., Kamisago, M., Momma, K., Katayama, H., Nakagawa, M., Fujiwara, Y., Matsushima, M., Mizuno, K., Tokuyama, M., Hirota, H., Muneuchi, J., Higashinakagawa, T., Matsuoka, R., 2007. Germline gain-of-function mutations in RAF1 cause Noonan syndrome. Nat. Genet. 39 (8 39), 1013–1017. https://doi.org/10.1038/ng2078.

Roberts, A.E., Allanson, J.E., Tartaglia, M., Gelb, B.D., 2013. Noonan syndrome. Lancet. https://doi.org/10.1016/S0140-6736(12)61023-X.

Scott, A., di Giosaffatte, N., Pinna, V., Daniele, P., Corno, S., Andreucci, E., Marozza, A., Sirchia, F., Tortora, G., Mangiameli, D., di Marco, C., Romagnoli, M., Donati, I., Zonta, A., Grosso, E., Giorgia Naretto, V., Mastromoro, G., Versacci, P., Pantaleoni, F., Clementina Radio, F., Mazza, T., Damante, G., Papi, L., Mattina, T., Giancotti, A., Pizzuti, A., Laberge, A.-M., Tartaglia, M., Delrue, M.-A., de Luca, A., 2021. When to test fetuses for RASopathies? Proposition from a systematic analysis of 352 multicenter cases and a postnatal cohort. Genet. Med. 23 https://doi.org/10.1038/s41436-020-01093-7.

Volpe, J.J., 2009. Brain injury in premature infants: a complex amalgam of destructive and developmental disturbances. Lancet Neurol. https://doi.org/10.1016/S1474-4422(08)70294-1.

Wilkinson, J.D., Lowe, A.M., Salbert, B.A., Sleeper, L.A., Colan, S.D., Cox, G.F., Towbin, J.A., Connuck, D.M., Messere, J.E., Lipshultz, S.E., 2012. Outcomes in children with Noonan syndrome and hypertrophic cardiomyopathy: a study from the Pediatric Cardiomyopathy Registry. Am. Heart J. 164, 442–448. https://doi.org/10.1016/J.AHJ.2012.04.018.